CHAPTER 5

RECONSTRUCTION OF AXISYMMETRIC AZIMUTHALLY POLARIZED ELECTROMAGNETIC LOCALIZED PULSED WAVE FIELDS

5.1 Introductory Remarks

Our work so far has been restricted to scalar-valued LW solutions of the scalar wave equation and the Klein-Gordon equation. In this chapter, we shall present a special class of infinite energy vector-valued LW solutions to Maxwell's equations, which will be referred to as *azimuthally polarized localized waves* (APLWs). These solutions will be derived directly from Maxwell's equations without the intervention of electromagnetic potentials. The reconstruction of these solutions will be addressed, as well as that of their time-limited counterparts.

5-2 Azimuthally Polarized Electromagnetic Fields

Conventional transverse electric $\left(TE_z\right)$ localized wave theory, expounded by Ziolkowski [27], is based on a vector magnetic Hertz potential $\boldsymbol{\pi_m} = \hat{a}_z\, \pi_m\left(\rho, z, t\right)$, with $\pi_m\left(\rho, z, t\right)$ governed by the scalar wave equation. Localized wave solutions to this equation, e.g., the MPS pulse, are used to compute the components $E_\phi\left(\rho, z, t\right)$, $H_\rho\left(\rho, z, t\right)$ and $H_z\left(\rho, z, t\right)$ of the corresponding localized electric and magnetic field intensities. The computation of these field components, although straightforward, results in very complex waveforms. As a consequence, the derivation of the electromagnetic energy density is very involved. So is the proof that the electromagnetic fields corresponding to the MPS solution of the scalar wave equation for $\pi_m\left(\rho, z, t\right)$ contain finite energy.

In what follows we demonstrate that $E_\phi(\rho,z,t)$ obeys a scalar equation different from the scalar wave equation for $\pi_m(\rho,z,t)$. However, it supports localized wave solutions analogous to the conventional FWM and MPS pulses. These solutions will be called azimuthally polarized localized waves (APLW). Once an APLW solution is found for $E_\phi(\rho,z,t)$, without an intermediate potential, the corresponding magnetic field intensity components $H_\rho(\rho,z,t)$ and $H_z(\rho,z,t)$ can be found from Maxwell's equations. There are several distinct advantages in our procedure: (i) exploitation of various types of localized waves at the level of the field $E_\phi(\rho,z,t)$ without the intervention of a potential function.; (ii) drastic reduction in the complexity of the computation of the magnetic field components;. (iii) a much easier computation of the electromagnetic energy density and Poynting vector; (iv) an easier check of the finiteness of the energy in the case of an APMPS pulse; (v) feasibility for a Huygens reconstruction of the localized electromagnetic fields.

Consider Maxwell's equations in free space:

$$\nabla\times\mathbf{E}(\mathbf{r},t)=-\mu_0\frac{\partial}{\partial t}\mathbf{H}(\mathbf{r},t), \tag{5.2.1a}$$

$$\nabla\times\mathbf{H}(\mathbf{r},t)=\varepsilon_0\frac{\partial}{\partial t}\mathbf{E}(\mathbf{r},t)+\mathbf{J}(\mathbf{r},t), \tag{5.2.1b}$$

$$\nabla\cdot\mathbf{E}(\mathbf{r},t)=\frac{\rho(\mathbf{r},t)}{\varepsilon_0}, \tag{5.2.1c}$$

$$\nabla\cdot\mathbf{H}(\mathbf{r},t)=0. \tag{5.2.1d}$$

The magnetic field intensity can be eliminated from these equations, giving rise to the following equation for the electric field intensity:

$$\nabla \times \nabla \times \mathbf{E}(\mathbf{r},t) + \frac{1}{c^2}\frac{\partial^2}{\partial t^2}\mathbf{E}(\mathbf{r},t) = -\mu_0 \frac{\partial}{\partial t}\mathbf{J}(\mathbf{r},t). \tag{5.2.2}$$

In a source-free region, this equation admits a zero-divergence solution of the form $\mathbf{E}(\mathbf{r},t) = \hat{a}_\phi E_\phi(\rho,z,t)$,

with $E_\phi(\rho,z,t)$ obeying the equation

$$\frac{1}{\rho}\frac{\partial}{\partial \rho}\left[\rho \frac{\partial}{\partial \rho} E_\phi(\rho,z,t)\right] - \frac{1}{\rho^2}E_\phi(\rho,z,t) + \frac{\partial^2}{\partial z^2}E_\phi(\rho,z,t) - \frac{1}{c^2}\frac{\partial^2}{\partial t^2}E_\phi(\rho,z,t) = 0 \tag{5.2.3}$$

in cylindrical coordinates. The term *azimuthal polarization* denotes a field propagating along z with the electric field $\mathbf{E}$ oriented along the ϕ direction. An axisymmetric, azimuthally polarized electric field intensity is of the form $\mathbf{E} = \hat{a}_\phi E_\phi(\rho,z,t)$. The corresponding magnetic field intensity has components $H_\rho(\rho,z,t)$ and $H_z(\rho,z,t)$. The azimuthally polarized state is familiar in fiber optics. The TE_{01} mode of a step-index optical fiber is a specific example [146]. The azimuthally polarized electromagnetic field is also of particular interest because of a recent experimental demonstration, whereby a broad area, concentric-circle-grating, surface-emitting (CCGSE) semiconductor laser radiates a near infrared, circularly symmetric, azimuthally polarized beam. Jordan and Hall [80,81] have developed a continuous wave (CW) paraxial equation for azimuthally polarized, axisymmetric fields and have compared the solutions of this equation to those of the more familiar scalar paraxial equation that yields linearly polarized Bessel-Gauss beams.

5.3 Azimuthally Polarized X Wave

Consider the Fourier-Hankel transform pair

$$\tilde{\tilde{E}}_{\phi}\left(\chi,k_z,\omega\right)=\int_{-\infty}^{\infty}dt\int_{-\infty}^{\infty}dz\int_{0}^{\infty}d\rho\,\rho J_1\left(\chi\rho\right)e^{-i\omega t}\,e^{ik_z z}E_{\phi}\left(\rho,z,t\right),\tag{5.3.1a}$$

$$E_{\phi}\left(\rho,z,t\right)=\frac{1}{(2\pi)^3}\int_{-\infty}^{\infty}d\omega\int_{-\infty}^{\infty}dk_z\int_{0}^{\infty}d\chi\,\chi J_1\left(\chi\rho\right)e^{i\omega t}\,e^{-ik_z z}\hat{E}_{\phi}\left(\chi,k_z,\omega\right).\tag{5.3.1b}$$

The insertion of the Hankel-Fourier transform of the electric field given in Eq. (5.3.1) into Eq. (5.2.3) leads to the dispersion relation

$$\left(\omega/c\right)^2-k_z^2-\chi^2=0.\ .\tag{5.3.2}$$

As a consequence, a representation for $E_{\phi}\left(\rho,z,t\right)$ can be written as follows [156]:

$$E_{\phi}\left(\rho,z,t\right)=\frac{1}{(2\pi)^3}\int_{-\infty}^{\infty}d\omega\int_{-\infty}^{\infty}dk_z\int_{0}^{\infty}d\chi\,\chi J_1\left(\chi\rho\right)e^{i\omega t}\,e^{-ik_z z}\delta\left(\left(\omega/c\right)^2-k_z^2-\chi^2\right)\hat{A}_0\left(\chi,k_z,\omega\right).\tag{5.3.3}$$

We consider a solution made up of superposition of plane waves moving in the positive z direction; specifically,

$$E_{\phi}\left(\rho,z,t\right)=\frac{1}{(2\pi)^3}\int_{0}^{\infty}d\omega\int_{0}^{\infty}dk_z\int_{0}^{\infty}d\chi\,\chi J_1\left(\chi\rho\right)e^{i\omega t}\,e^{-ik_z z}\delta\left(\left(\omega/c\right)^2-k_z^2-\chi^2\right)\hat{B}_0\left(\chi,k_z,\omega\right),\tag{5.3.4}$$

Integrating over ω, we obtain

$$E_{\phi}\left(\rho,z,t\right)=\frac{1}{(2\pi)^3}\int_{0}^{\infty}dk_z\int_{0}^{\infty}\chi d\chi J_1\left(\chi\rho\right)e^{-ik_z\left(z-ct\left(\sqrt{\chi^2+k_z^2}/k_z\right)\right)}\hat{D}_0\left(\chi,k_z\right).\tag{5.3.5}$$

To generate an X wave, we introduce the constraint

$$c\frac{\sqrt{\chi^2+k_z^2}}{k_z}=\upsilon\,, \tag{5.3.6}$$

where υ is a constant superluminal speed $(\upsilon > c)$. Alternatively, we have

$$k_z=\frac{\chi}{\sqrt{(\upsilon/c)^2-1}}\equiv\gamma\chi\,, \tag{5.3.7}$$

Substituting this constraint into Eq. (5.3.5), we obtain

$$E_\phi(\rho,z,t)=\frac{1}{(2\pi)^3}\int_0^\infty d\chi\,\chi\,J_1(\chi\rho)e^{-i\gamma\chi(z-\upsilon t)}\hat{E}_0(\chi)\,. \tag{5.3.8}$$

With the specific choice

$$\hat{E}_0(\chi)=e^{-a_1\chi};\;\; a_1>0\,, \tag{5.3.9}$$

we can use Eq. (6.623.1) in [144] to obtain the azimuthally polarized X wave solution

$$E_\phi^{APXW}(\rho,z,t)=\frac{1}{(2\pi)^3}\frac{2\Gamma(3/2)}{\sqrt{\pi}}\frac{\rho}{\left\{\rho^2+\left[a_1+i\gamma(z-\upsilon t)\right]^2\right\}^{3/2}}\,. \tag{5.3.10}$$

In contradistinction to FWM-like pulses, we can derive explicit expressions for the magnetic components using the following relationships [156]:

$$H_\rho(\rho,z,t)=\frac{1}{\mu_0}\int^t d\tau\frac{\partial}{\partial z}E_\phi(\rho,z,\tau)\,, \tag{5.3.11a}$$

$$H_\phi(\rho,z,t)=0\,, \tag{5.3.11b}$$

$$H_z(\rho,z,t) = -\frac{1}{\mu_0}\int^{t} d\tau \frac{1}{\rho}\frac{\partial}{\partial\rho}\left[\rho E_\phi(\rho,z,\tau)\right]. \tag{5.3.11c}$$

Corresponding to the electric field intensity given in Eq. (5.3.11), we obtain

$$H_\rho^{APXW}(\rho,z,t) = \frac{-A\rho}{\mu_0 \upsilon\left\{\rho^2 + \left[a_1 + i\gamma(z-\upsilon t)\right]^2\right\}^{3/2}}, \tag{5.3.12a}$$

$$H_z^{APXW}(\rho,z,t) = \frac{iA\left(a_1 + i\gamma(z-\upsilon t)\right)}{\mu_0 \gamma\upsilon\left\{\rho^2 + \left[a_1 + i\gamma(z-\upsilon t)\right]^2\right\}^{3/2}} \tag{5.3.12b}$$

for the magnetic field intensity components. Here, $A = \dfrac{2\Gamma(3/2)}{(2\pi)^3\sqrt{\pi}}$

5.4 Reconstruction of Azimuthally Polarized X Waves in the Time domain

By analogy to the reconstruction of scalar-valued localized waves considered in Chapter 2, vector-valued azimuthally polarized X waves can be reconstructed by means of Kirchhoff's surface integral representation (KSIR). The required quantities for the numerical implementation of the reconstruction are the tangential electromagnetic fields and their derivatives with respect to time and space defined over the source plane. The radiated fields away from the aperture can be evaluated by means of the time-domain formulation of KSIR as follows [143]:

$$\begin{aligned}\mathbf{E} = -\frac{1}{4\pi}\int_V \left[\mu\frac{\partial[\mathbf{J}]}{\partial t} + \frac{1}{\varepsilon_0}\mathrm{grad}[\rho]\right]\frac{d\tau'}{R} - \frac{1}{4\pi}\int_{S'}\left\{\left(\hat{n}\times[\mathbf{E}]\right)\times\mathrm{grad}'\frac{1}{R} - \frac{1}{cR}\left(\hat{n}\times\left[\frac{\partial\mathbf{E}}{\partial t}\right]\right)\right. \\ \left.\times\,\mathrm{grad}'R + \left(\hat{n}.[\mathbf{E}]\right)\mathrm{grad}'\frac{1}{R} - \frac{1}{cR}\left(\hat{n}\cdot\left[\frac{\partial\mathbf{E}}{\partial t}\right]\right)\mathrm{grad}'R - \frac{1}{R}\hat{n}\times\left[\frac{\partial\mathbf{B}}{\partial t}\right]\right\}dS',\end{aligned} \tag{5.4.1}$$

$$\mathbf{H} = \text{curl}\ \frac{1}{4\pi}\int_V \frac{[\mathbf{J}]}{R}d\tau' - \frac{1}{4\pi}\int_{S'}\left\{\left(\hat{n}\times[\mathbf{H}]\right)\times\text{grad}'\frac{1}{R} - \frac{1}{cR}\left(\hat{n}\times\left[\frac{\partial\mathbf{H}}{\partial t}\right]\right)\times\text{grad}'R\right.$$
$$\left. + \left(\hat{n}\cdot[\mathbf{H}]\right)\ \text{grad}'\frac{1}{R} - \frac{1}{cR}\left(\hat{n}\cdot\left[\frac{\partial\mathbf{H}}{\partial t}\right]\right)\text{grad}'R + \frac{1}{R}\hat{n}\times\left[\frac{\partial\mathbf{D}}{\partial t}\right]\right\}dS', \tag{5.4.2}$$

where $\mathbf{D} = \varepsilon_0\mathbf{E}$ and S is the surface bounding the volume V. The rectangular brackets denote that the variables contained within them are to be evaluated at the retarded time $t' = t - (R/c)$, where $R = |\mathbf{r} - \mathbf{r}'|$.

We have two types of sources: (1) Initial electromagnetic fields illuminating the aperture and (2) real current sources driving the dynamic antenna. We shall use the equivalence between the surface currents and fields to guide us to an adequate choice of the source currents. The current in the ϕ direction can be determined from the magnetic field component as follows:

$$\mathbf{J} = \hat{n}\times H_\rho\hat{\rho} = H_\rho\hat{\phi} \tag{5.4.3}$$

Examining Eq. (5.3.10), we note that the electric field component E_ϕ has zero value along the z-axis $(\rho = 0)$. Its differentiation with respect to ρ gives a maximum value that occurs at $\rho = a_1/\sqrt{2}$. As a result, in our numerical work we have computed the reconstructed field at observing points with coordinates $\left(a_1/\sqrt{2}, 0, z = \upsilon t\right)$.

5-5 Reconstruction of Azimuthally Polarized X Waves in the Frequency Domain

The frequency domain expressions of the KSIR [143] corresponding to Eqs. (5.4.1) and (5.4.2) can be written as

$$\mathbf{E}(\rho,\phi,z,\omega)=\frac{1}{4\pi}\int_{S'}\left[-i\omega\mu\psi(\hat{n}\times\mathbf{H})\div(\hat{n}\times\mathbf{E})\times\nabla\psi+(\hat{n}.\mathbf{E})\nabla\psi\right]dS', \tag{5.5.1}$$

$$\mathbf{H}(\rho,\phi,z,\omega)=\frac{1}{4\pi}\int_{S'}\left[i\omega\varepsilon\psi(\hat{n}\times\mathbf{E})\div(\hat{n}\times\mathbf{H})\times\nabla\psi+(\hat{n}.\mathbf{H})\nabla\psi\right]dS', \tag{5.5.2}$$

where $\hat{n}$ is the unit vector normal to the source plane and

$$\psi=\frac{e^{-ikR}}{R},\ k=\omega/c,\ \ R=\sqrt{\rho^2+\rho'^2-2\rho\rho'\cos(\phi-\phi')+(z-z')^2}\,. \tag{5.5.3}$$

We deal with the fields E_ϕ, H_ρ and H_z as a TE_z mode system defined in a cylindrical coordinate system. Consequently, we have

$$\begin{aligned}\nabla\psi&=\frac{\partial\psi}{\partial\rho}\hat{\rho}+\frac{\partial\psi}{\rho\partial\phi}\hat{\phi}+\frac{\partial\psi}{\partial z}\hat{z}\\&=-\left[\frac{1}{R}+ik\right]\frac{e^{-ikR}}{R}\left[\frac{\rho-\rho'\cos\phi'}{R}\hat{\rho}-\frac{\rho'\sin\phi'}{R}\hat{\phi}+\frac{z-z'}{R}\hat{z}\right].\end{aligned} \tag{5.5.4}$$

In this expression, we have set $\phi=0$ due to the symmetry of the observing point with respect to the discrete annular sections distributed over the source plane. Equating the field components for both sides of Eq. (5.5.1), after plugging Eq. (5.5.4) into it, leads to the electric field component in the ϕ direction

$$E_\phi(\rho,\omega,z)=\frac{1}{4\pi}\int_{S'}\left[-i\omega\mu\frac{e^{-jkR}}{R}H_\rho(\rho',\omega)-\frac{e^{-ikR}}{R}E_\phi(\rho',\omega)\left\{\frac{1}{R}+ik\right\}\frac{z-z'}{R}\right]dS', \tag{5.5.5}$$

where the differential area on the source plane is defined as $dS'=\rho' d\rho' d\phi'$. Based on Eqs. (5.3.10) and (5.3.12a), the electric field temporal spectrum component in the second term of the integrand can be written in terms of the magnetic one in the first term as

$$E_\phi(\rho',\omega) = \int_0^\infty E_\phi(\rho',t)e^{-i\omega t}dt = \int_0^\infty J_1(\chi\rho')\chi d\chi E_\phi(\chi,\omega)$$

$$= \frac{\omega A}{2\pi(\gamma\upsilon)^2} e^{-\omega a_1/\gamma\upsilon} J_1\left(\frac{\omega}{\gamma\upsilon}\rho'\right) = \mu_0 \upsilon H_\rho(\rho',\omega), \tag{5.5.6a}$$

where

$$E_\phi(\chi,\omega) = \frac{A}{(2\pi)^2} e^{-a_1\chi}\delta(\omega - \gamma\upsilon\chi). \tag{5.5.6b}$$

Our main interest here is to focus on the evaluation of the electric field component E_ϕ from which we can obtain the other two components H_ρ, H_z using Eqs. (5.3.11a) and (5.3.11c), respectively.

5.6 Time-Limited Azimuthally Polarized X-Waves

A time-limited version of the azimuthally polarized X wave electric field given in Eq. (5.3.10) is given as

$$E_\phi^{APXW}(\rho,0,t) = \frac{A\rho}{\left\{\rho^2 + \left(a_1 - i\gamma\upsilon t\right)^2\right\}^{3/2}} e^{-t^2/T^2}. \tag{5.6.1}$$

on the aperture plane $z = 0$. Its spatio-temporal spectrum can be computed as follows:

$$\hat{E}_\phi(\chi,\omega) = \int_0^\infty dt \int_0^\infty d\rho\rho J_1(\chi\rho)e^{-i\omega t} E_\phi(\rho,0,t)$$

$$= \int_0^\infty dt \int_0^\infty d\rho\rho J_1(\chi\rho)e^{-i\omega t} \frac{A\rho}{\left\{\rho^2 + \left(a_1 - i\gamma\upsilon t\right)^2\right\}^{3/2}} e^{-t^2/T^2}. \tag{5.6.2}$$

The integrations over the variables ρ and t can be performed using Eqs. (6.565.2) and (3.324.3) in Ref. [144]. The final result is given by

$$E_{\phi}(\chi,\omega) = 2\sqrt{\pi}TAe^{-a_1\chi}e^{-T^2(\omega-\gamma\upsilon\chi)^2}, \tag{5.6.3}$$

The electric field in front of the source plane can be determined from the Weyl representation

$$E_{\phi}(\rho,z,t) = \frac{\sqrt{\pi}cTA}{(2\pi)^2}\int_0^{\infty}\chi d\chi J_1(\chi\rho)\int_0^{\infty}dke^{-a_1\chi}e^{-T^2y_0^2\left(k/y_1-\chi\right)^2}e^{-i\left(\sqrt{k^2-\chi^2}z-kct\right)}, \tag{5.6.4}$$

Here, we are using the notation

$$\gamma = \sinh\beta,\ \ \upsilon = c\coth\beta;\ y_1 = \cosh\beta;\ y_0 = c\cosh\beta. \tag{5.6.5}$$

Next, we substitute Eq. (5.6.4) into Eqs. (5.3.11a) and (5.3.11c) in order to compute the corresponding magnetic field intensity components. They can be expressed as

$$H_{\rho}(\rho,z,t) = B\int_0^{\infty}\chi d\chi J_1(\chi\rho)\int_0^{\infty}dk\,\frac{\sqrt{k^2-\chi^2}}{kc}e^{-a_1\chi}e^{-T^2y_0^2\left(k/y_1-\chi\right)^2}e^{-i\left(\sqrt{k^2-\chi^2}z-kct\right)}, \tag{5.6.6}$$

$$H_z(\rho,z,t) = B\int_0^{\infty}\chi^2 d\chi J_0(\chi\rho)\int_0^{\infty}dk\,\frac{1}{ikc}e^{-a_1\chi}e^{-T^2y_0^2\left(k/y_1-\chi\right)^2}e^{-i\left(\sqrt{k^2-\chi^2}z-kct\right)}. \tag{5.6.7}$$

where $B = \dfrac{\sqrt{\pi}cTA}{(2\pi)^2\mu_0}$

In order to avoid evanescent fields, the propagation constant k_z should be real. For this reason, the integration over the wave number k should take the minimum value $k = \chi$. Consequently, we rewrite the previous expressions as follows:

$$E_\phi(\rho,z,t) = B\mu_0 \int_0^\infty \chi d\chi J_1(\chi\rho) \int_\chi^\infty dk e^{-a_1\chi} e^{-T^2 y_0^2 \left(k/y_1 - \chi\right)^2} e^{-i\left(\sqrt{k^2-\chi^2}z - kct\right)}, \tag{5.6.8}$$

$$H_\rho(\rho,z,t) = B\int_0^\infty \chi d\chi J_1(\chi\rho) \int_\chi^\infty dk \frac{\sqrt{k^2-\chi^2}}{kc} e^{-a_1\chi} e^{-T^2 y_0^2 \left(k/y_1 - \chi\right)^2} e^{-i\left(\sqrt{k^2-\chi^2}z - kct\right)}, \tag{5.6.9}$$

$$H_z(\rho,z,t) = B\int_0^\infty \chi^2 d\chi J_0(\chi\rho) \int_\chi^\infty dk \frac{1}{ikc} e^{-a_1\chi} e^{-T^2 y_0^2 \left(k/y_1 - \chi\right)^2} e^{-i\left(\sqrt{k^2-\chi^2}z - kct\right)}. \tag{5.6.10}$$

5.7 Numerical Results

The variation of the current density $\left(\text{equivalent to } H_\rho\right)$ with ρ at different instants is depicted in Fig. 5.1. Figure 5.2 shows the time history of the electric field E_ϕ at different ρ values. We notice from these two graphs that the peaks of H_ρ and E_ϕ over the source plane move with lower amplitudes away from the center as t increases. This illustrates the dynamic behavior of the aperture over which the discrete sources are distributed. Additionally, the energy density contained in the localized source decreases as the radius of the aperture increases. The decay of the centroid field value of H_z with distance z for a time-limited azimuthally polarized X wave is shown in Fig. 5.3. It is clear that the decay rate is inversely proportional to the excitation time T, or equivalently the effective radius of the aperture. A comparison between the time history of the electric field component E_ϕ generated from a finite aperture of radius $R_{\max} = 4.8$ m and that of the exact field is shown in Fig. 5.4 for $z = 50$ m and $\rho = 0.106$ m. The reconstructed field is found by means of KSIR in the frequency domain, together with an inverse FFT. A comparison of the time history of the electric field component E_ϕ generated from a time-limited aperture

$(T = 0.04$ ns$)$ using the Weyl representation and that of the exact field is shown in Fig. 5.5 for $z = 50$ m and $\rho = 0.106$ m. We have selected the observing point for E_ϕ to be at $\rho = a_1/\sqrt{2} = 0.106$ m because it has a zero value along the z-axis. In contradistinction, H_z has its maximum value at $\rho = 0$. Figure. 5.6 provided a comparison between the time history of H_z generated from a time-limited aperture $(T = 0.04$ ns$)$ and that of the exact field at $z = 250$ m and $\rho = 0$. For the numerical results presented so far, we have used the values of the tangential field components and their derivatives on the source plane. However, in Fig. 5.7 we present a comparison of the time history of the exact field E_ϕ and that of a reconstructed field due to a localized current source distributed over the aperture plane. The distance from the aperture equals 250 m and $\rho = 0.106$ m.

5.8 Concluding Remarks

We have carried out numerically the reconstruction of vector-valued azimuthally polarized X wave fields using Kirchhoff's surface integral representation, with localized currents and tangential field components as exciting sources. Moreover, we have computed the time-limited versions of the azimuthally localized X waves by means of the Weyl representation with finite excitation time. Because of their distinctive characteristics, azimuthally polarized X wave fields may find applications in remote sensing, medical imaging, secure communications, directed energy transfer and ultra-wideband radars. Hopefully, our work sheds some light on the possibility of generating these type of localized fields, especially in view of recent advances in generating sources of ultra-wide bandwidth electromagnetic energy.

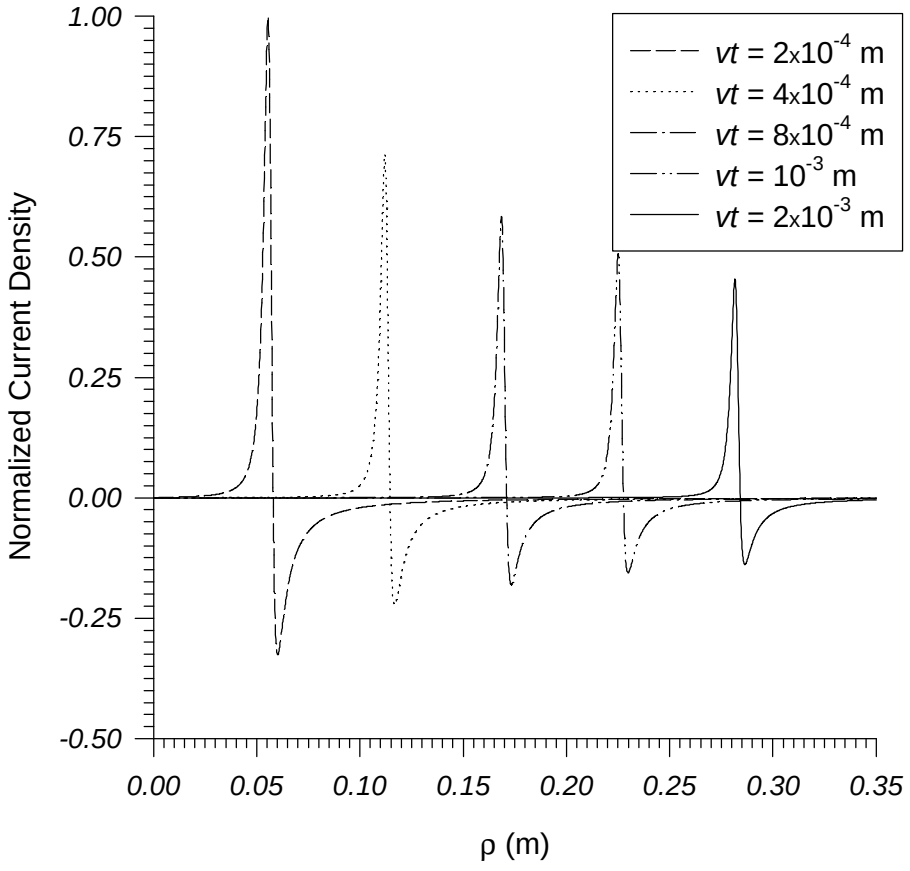

Figure 5.1: Variation of the current density with the transverse direction ρ at different instants.

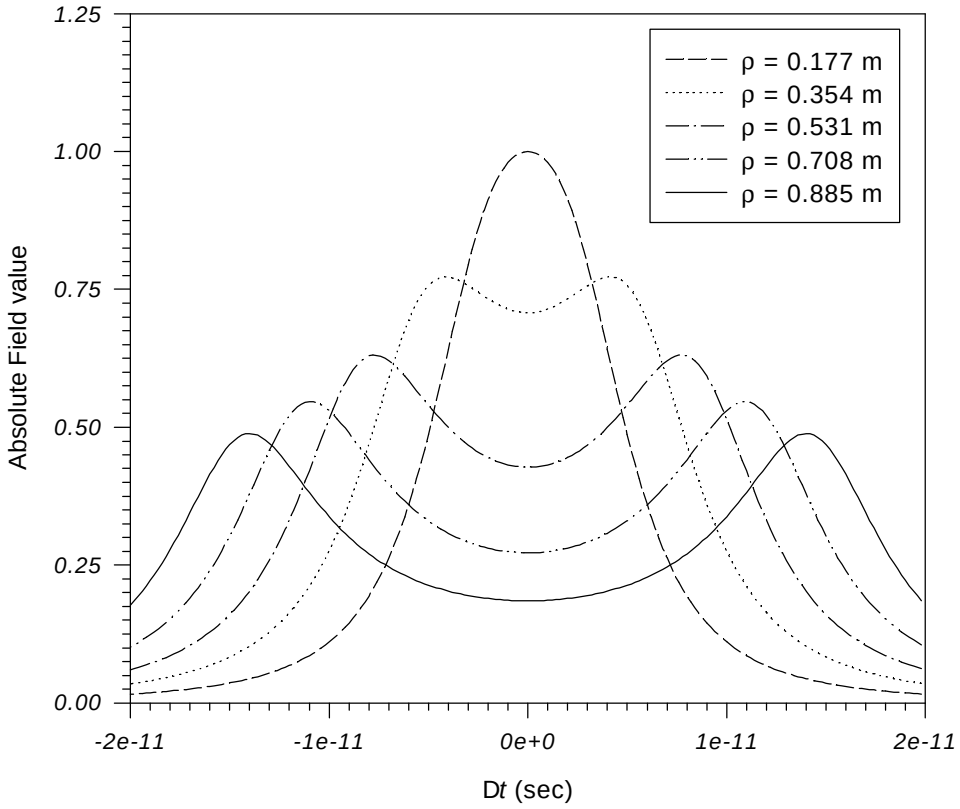

Figure 5.2: The time history of the field value E_ϕ on the source plane at different radii of the annular sections $\rho = 0.177,\ 0.354,\ 0.531,\ 0.708,\ 0.885\text{m}$. The parameters of the pulse are: $a_1 = 0.25,\ \beta = 6$.

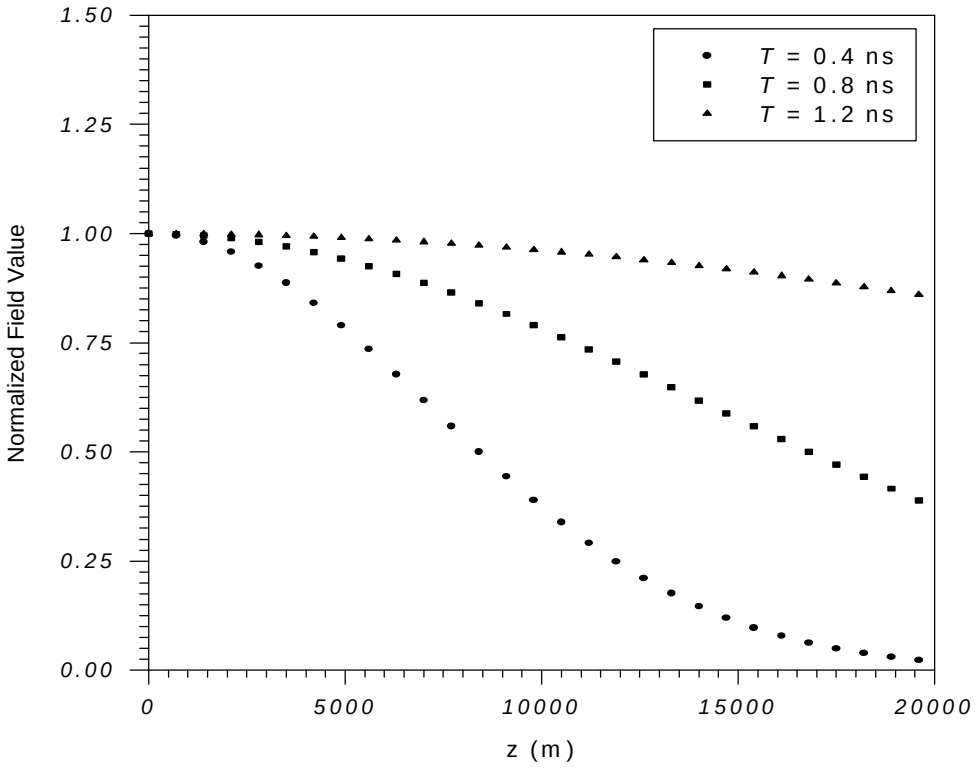

Figure 5.3: The decay of the centroid field value of a finite time azimuthally polarized magnetic field H_z with the distance z in front of the source plane. It is clear that the decay is inversely proportional to the excitation time T.

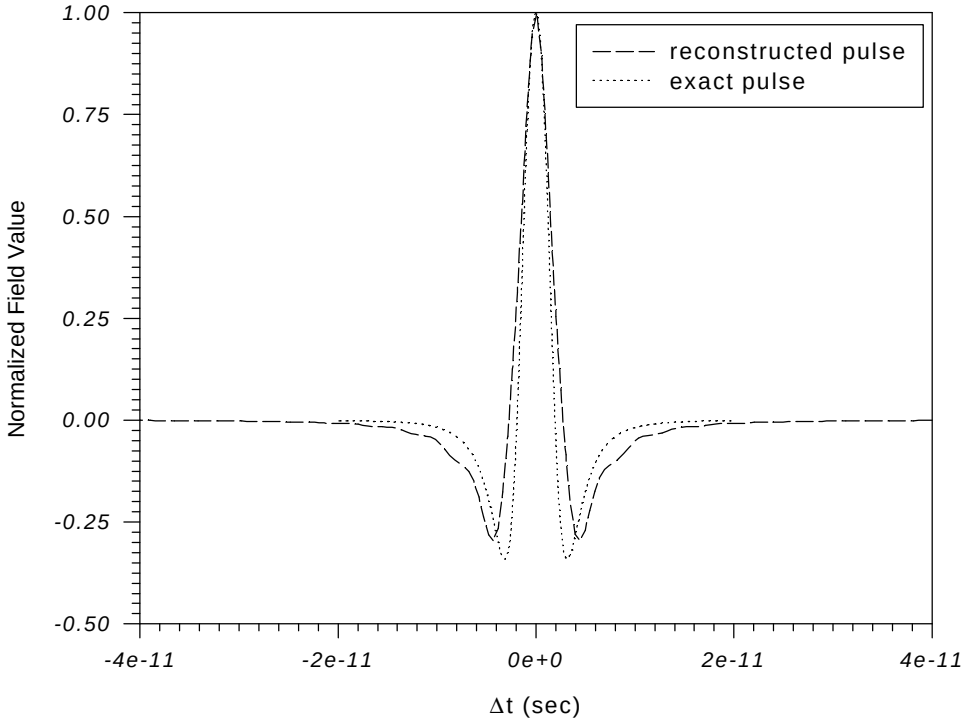

Figure 5.4: Comparison between the time history of the electric field component E_ϕ generated from finite aperture with radius $R_{\max} = 4.8\text{m}$ and the exact one at $z = 50\text{m}$, $r = 0.106\ \text{m}$. We have applied the vector Kirchhoff integral and then IFFT.

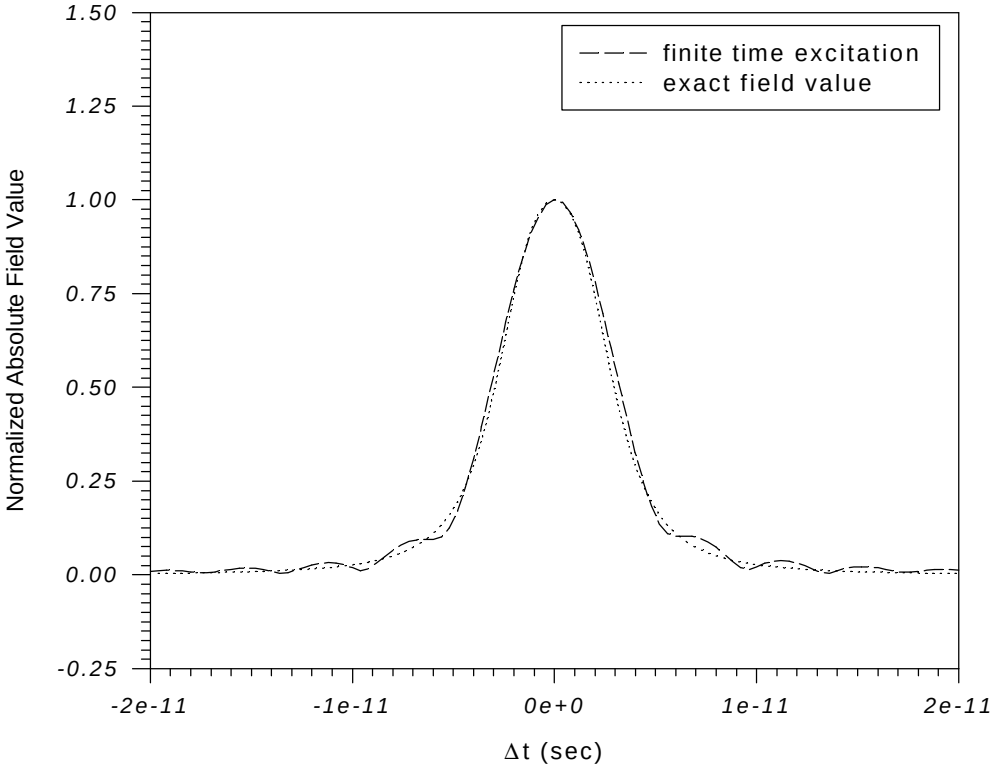

Figure 5.5: Comparison between the time history of the electric field component E_ϕ generated from time-limited aperture $4T$, $T = 0.04\text{ns}$, $a_1 = 0.15$ by using Weyl representation and the exact one at $z = 50\text{m}$, $\rho = 0.106\text{ m}$.

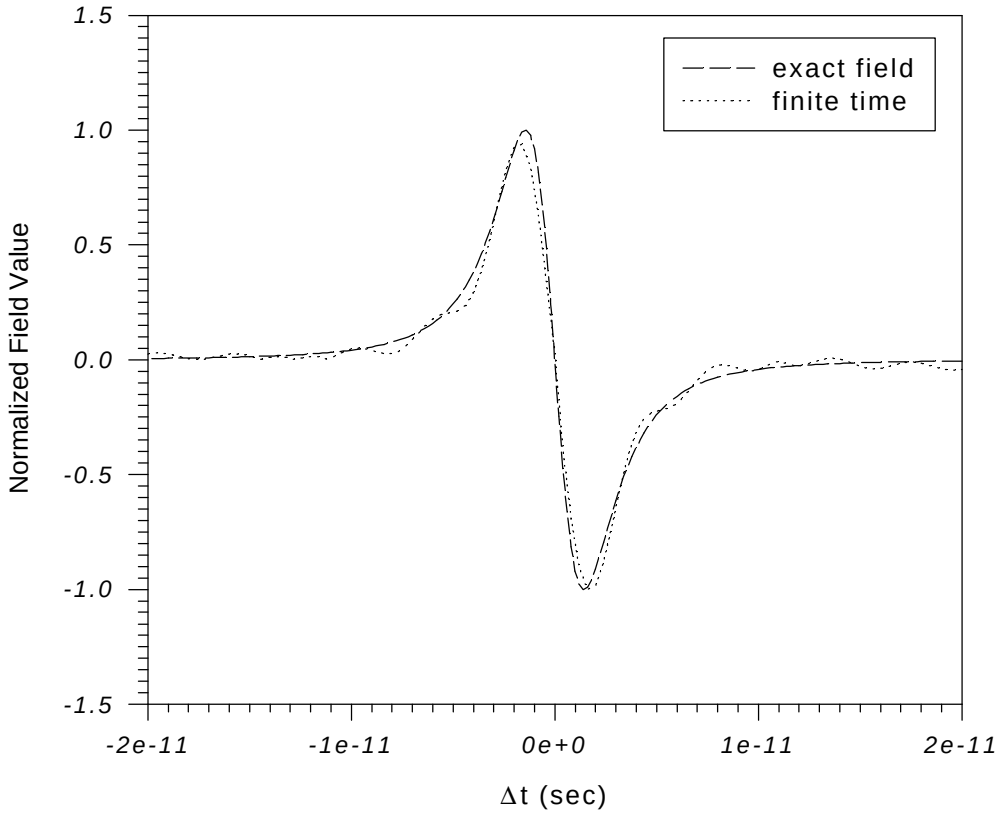

Figure 5.6: The comparison between the time history of the magnetic field component H_z generated from finite time aperture with radius $R_{\max} = 4.8$ m, $T = 0.04$ns, $\beta = 6$ and the exact one at $z = 250$ m, $\rho = 0$.

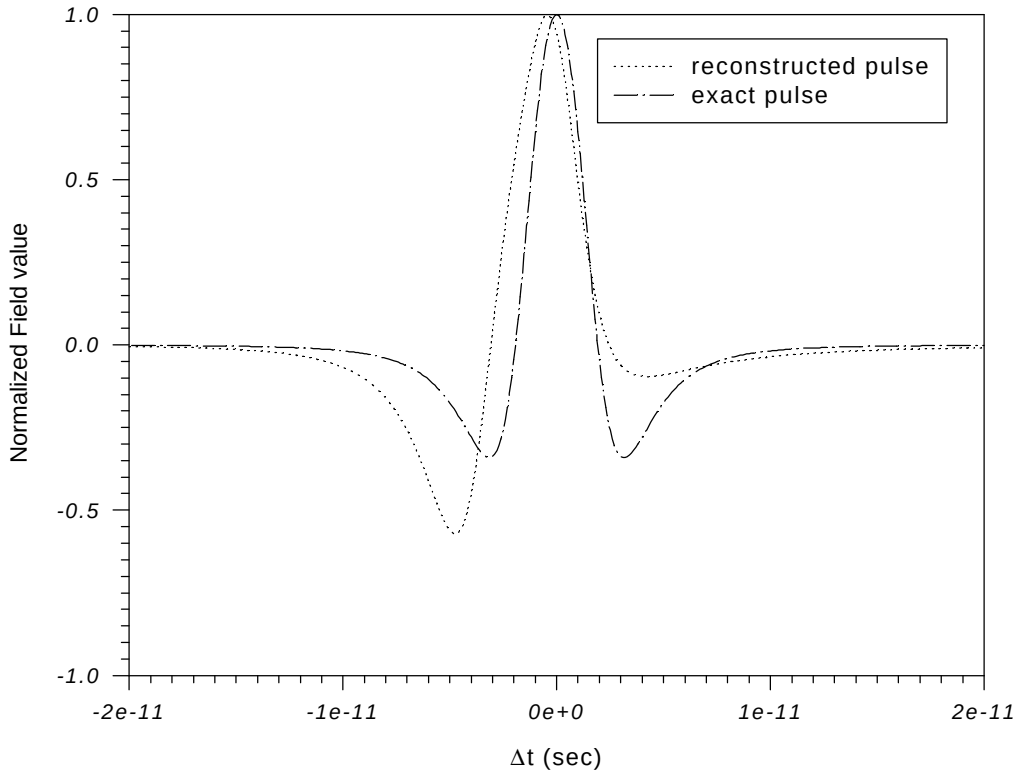

Figure 5.7: The comparison between the time history of the reconstructed field E_ϕ at $z = 250$ m, $\rho = 0.106$ m due to localized current source distributed on the source plane and the exact one. The radius of the aperture is $R_{\max} = 4.8$m.